Poly(ε-caprolactone) Grafted Dextran Biodegradable Electrospun Matrix: A Novel Scaffold for Tissue Engineering

Madhab Prasad Bajgai,[1] Santosh Aryal,[2] Shanta Raj Bhattarai,[1] K. C. Remant Bahadur,[3] Kawn-Woo Kim,[1] Hak Yong Kim[4]

[1]*Department of Bionanosystem Engineering, Chonbuk National University, Jeonju 561-756, Republic of Korea*
[2]*Center for Healthcare Technology Development, Chonbuk National University, Jeonju 561-756, Republic of Korea*
[3]*Department of Advance Organic Material Science and Engineering, Kyungpook National University, Daegu 702-701, Republic of Korea*
[4]*Department of Textile Engineering, Chonbuk National University, Chonju 561-756, Republic of Korea*

Received 28 July 2007; accepted 20 November 2007
DOI 10.1002/app.27825
Published online 23 January 2008 in Wiley InterScience (www.interscience.wiley.com).

ABSTRACT: The main objective of the present work was to fabricate poly(ε-caprolactone) grafted dextran (PGD) electrospun matrix (matrix) and to investigate the scaffold potential in tissue engineering application. In this work, at first we synthesized PGD polymer via ring opening polymerization (ROP), and with predetermined electrospinning conditions, nanofibrous matrix with high molecular weight PGD (PGD-50, M_w = 45,500) has been successfully fabricated for the first time. Mouse osteoblast like cells, MC3T3 was used to test biocompatibility, assays of cell adhesion, survival, and effects on cell morphology of the matrix. The data demonstrate that PGD-50 matrix represent a suitable substrate for supporting cell proliferation, process outgrowth and migration and as such would be a good material for artificial extra cellular matrix. © 2008 Wiley Periodicals, Inc. J Appl Polym Sci 108: 1447–1454, 2008

Key words: biomaterials; biodegradable; matrix; polyester; polysaccharides

INTRODUCTION

Electrospinning has been employed as a versatile technique to produce polymeric fibrous substrates for cell culture and tissue engineering applications.[1–3] Random or aligned nanofiber matrix with an average diameter ranging from 100 nm to over 1 μm has been prepared through the control of various electrospinning parameters.[2,4,5] Several studies have shown that these fibrous scaffolds can enhance cellular responses like cell adhesion and cell phenotype maintenance.[3,6–10] As cells adjust their shape according to morphological cues such as matrix texture (architecture and topography), high porosity stimulates the formation of fiber directed 3D cell structure, resulting in an integrated spheroid-nanofiber construct.[7,11,12] However, the choice of polymer is very important along with structural biocompatibility. With increasing interest in the use of biodegradable polymers in the area of reconstructive surgery, extensive research has been carried out. Synthetic biodegradable materials including polylactide, polyglycolide, poly(lactide-*co*-glycolide), and poly(ε-caprolactone) (PCL) are the frequently used polymers in biomedical fields owing to their superior mechanical properties.[7,10] However, cell affinity toward synthetic polymers is generally poor due to their low hydrophilicity and lack of surface cell recognition sites.[3,10] Furthermore, other transport issues including nutrient delivery, waste removal, exclusion of materials or cells, and protein transport are also influenced disadvantageously by the hydrophobicity of the scaffold.[9,13–15] Particularly, to improve the cell affinity of aliphatic polyesters, many efforts have been directed to modify their surface properties by adjusting the hydrophilicity/hydrophobicity, surface energy, surface charge, and surface roughness.[13] One of the possible and promising approaches to overcome aforesaid difficulty is to introduce hydrophilic segments into the aliphatic polyester. Though the electrospun PCL mats mimic the identity of extra cellular matrix (ECM) in living tissues, its hydrophobicity supervene in low cell

Correspondence to: H. Y. Kim (khy@moak.chonbuk.ac.kr).
Contract grant sponsor: the Korean Research Foundation; contract grant number: KRF2007-211-D00032.
Contract grant sponsor: the Ministry of Commerce, Industry and Energy Department and Regional Research Centers Program of the Korean Ministry of Educational and Human Resources Development through the Center for Healthcare Technology Development, Chonbuk National University, Jeonju 562-756, Republic of Korea; contract grant number: 10028211.

loading in the initial step of cell culture and diminution in the ability of cell adhesion, migration, proliferation, and differentiation.[10,15,16] So, there is an urgent need to develop hydrophilicity of hydrophobic biodegradable and biocompatible polymers to make an ideal scaffold for tissue engineering.[7,10] Our research group has already been investigated, one of the feasible methods to improve the hydrophilicity of PCL scaffold by blending system with hydrophilic polyethylene glycol (PEG) or polyvinyl alcohol (PVA).[4,10] Both PEG and PVA are excellent biocompatible polymers; and in the way that they have been FDA approved. Even though PVA is the only carbon–carbon backbone polymer that is biodegradable under both aerobic and anaerobic conditions, the degradation rate under natural environmental conditions is too slow.[17] Like wise the nondegradable ether bonds on PEG limits its application in specialized aims like controlled degradation.[18] For this reason, chemical modifications of these polymers with other biodegradable moieties are most promising approaches to improve not only the poor biodegradability of PVA or PEG but also to enhance the biodegradability of combined moiety by their hydroxyl functions attract aqueous environment.[17,18] Meanwhile, blending system with these polymers enumerate problems of continuous leaching out of hydrophilic parts from the matrix, makes the system dirty and destroy the structural integrity.

To develop an ideal scaffold for tissue engineering, physical (mechanical, thermal, structural) and chemical (functional moieties, biodegradability) factors of the scaffold surface are equally important.[1] Nevertheless it is very important to obtain a sufficient mass of seeded cells for uniform distribution through out the scaffold.[16] For this purpose, polysaccharides are interesting materials since their carbohydrate moieties interact with or are integral components of many cell adhesion molecules and matrix glycoprotein.[14–16]

Among the various biodegradable polymers, our material of interest is PCL owing to its excellent mechanical property and biocompatibility.[15,16] Hence, the matrix of PCL grafted polysaccharide can be a promising material that allows adequate mechanical properties with specific tissue and cell compatibility so that the scaffold degradation rate match with the growth rate of the regenerative tissue.[16,19]

Focusing above issue, we select PCL grafted dextran (natural and hydrophilic) polymer (PGD) as a starting block copolymer to overcome the low hydrophilicity of PCL and to improve poor mechanical properties of dextran so as to make a better scaffold for tissue engineering. In particular, owing to low mechanical stability and spinnability of biopolymer (polysaccharide) and for the fabrication of a nanofiberous 3D structure that mimics the natural ECM and provides a path for the reasonable proliferation of cells, PGD was synthesized by controlled grafting of PCL on the backbone of dextran. The proposed polymer not only gives a mechanical support to proliferate the cells but also governs the transport of O_2 through its porous structure. For the purpose, we have optimized and selected PGD-50 as a choice material for the fabrication of desired 3D nanofibres. Although, synthesis of PGD and their application for drug delivery has been reported elsewhere,[20–22] but the fabrication of nanomatrix and their application in tissue engineering has not been reported yet.

EXPERIMENTAL

Materials

Dextran (*Leuconostoc mesenteroides*, average M_w = 8500–11,500), ε-caprolactone (ε-CL), 1,1,1,3,3,3-hexamethyldisilazane (HMDS) (99.9%), triethylamine (99%), and stannous 2-ethyl hexanoate [$Sn(oct)_2$] were purchased from Sigma-Aldrich Inc., USA and used as received. All the other chemicals used in this research were purchased from Showa Chemical Ltd., Japan.

Synthesis of poly(ε-caprolactone) grafted dextran

Graft copolymer was synthesized as reported earlier.[20–22] Briefly, dextran was dissolved in dimethyl sulfoxide (10 wt % dextran) along with the addition of desired quantity of triethylamine and HMDS under a nitrogen flow with previously dried syringes. The reaction condition was kept at 60°C for 48 h. Meantime, 8 mL of tetrahydrofuran (THF) and 5 mL of toluene were added just after 4 h of reaction proceeded so as to make the reaction condition homogenous. After the completion of the reaction, the silylated dextran was precipitated in cold water; vacuum dried, and finally distilled azeotropically in toluene. Protection yields were calculated by ^{1}H NMR as described earlier.[19]

Further, ring opening polymerization (ROP) of ε-CL was performed in a previously dried three-necked round-bottom flask equipped with a stopcock and a rubber septum, purged with nitrogen. During the process, silylated dextran, which acts as a macro initiator, subjected for the ROP of ε-CL in toluene (10 wt % silylated dextran) in presence of stannous octoate [$Sn(Oct)_2$] as a catalyst with different feeding molar ratio (Table I). The polymerization was carried under nitrogen at 130°C for 72 h. The reaction product was recovered by precipitation in heptane, filtration, and dried under vacuum. PCL weight fraction (F_{PCL}) in the graft copolymers was determined by ^{1}H NMR (Table I) as described elsewhere.[17] Finally, silylated graft copolymers were dis-

TABLE I
Characteristic Feature of the Synthesized Polymer

Sample	Feed Ratio CL/OH	M_w	F_{PCL} ^{1}H NMR	T_{d^1} (°C)	T_{d^2} (°C)
PGE-20	20	14,100	0.94	355	420
PGD-30	30	20,300	0.96	427	–
PGD-50	50	45,500	0.98	430	–

solved in THF (10 wt % PCL-grafted silylated dextran) along with the addition of a slight excess of aqueous 0.1*M* HCl with respect to the number of -$OSiMe_3$ functions. After 2 h, the deprotected copolymers were recovered by precipitation in heptane and dried under vacuum and characterized. We synthesized three different products of PGD (PGD-20, PGD-30, and PGD-50) with different molecular weights as described in Table I.

Fabrication of PGD-50 electrospun matrix (PGD-50 matrix)

Reported knowledge of electrospinning work done in our laboratory of various polymers, all electrospinning parameter including applied voltage, distance between the needle tip (anode) and collector (cathode), solution flow rate, collector material, syringe and needle configuration, translation speed, and rotational speed were kept constant.[3,10] Solution of PGD-50 (25 wt %) in methylene chloride/dimethyl formamide (MC/DMF) (80/20) was selected for bead free PGD-50 electrospun fibers (Table II). The final viscosity of the above solution was determined as 419 cp (50 rpm, torque 3.15%). The electrospinning set up employed in this study is similar to that reported in previous study.[3,10] The polymer solution prepared as selected above is fed into 5 mL disposable syringe fitted with a pipette tip of 0.5 mm in diameter. The solution feed was driven by the gravity and the speed was controlled by the tilt angle of the syringe. Briefly, a DC voltage of 15 kV (High DC power supply, Del Electronics Corp.) was applied between the syringe tip and a cylindrical collector covered with aluminum foil. The cylinder had a diameter of 7 cm and was driven by a DC motor with controllable speed. The typical distance between the syringe tip and the grounded collector was 12 cm and the flow rate obtained was 1 mL/h. All the spinning experiments were performed at room temperature. The as-spun nanofibers were dried under vacuum at room temperature.

Preparation of cells and cell-matrix interaction

Mouse osteoblast like cells, MC3T3 (the Korean Cell Line Bank, Seoul, Korea), were maintained in Minimum Essential Medium (MEM) (Life Technologies, Co., USA) supplemented with 10% FBS, 300 μg/mL L-glutamine, 100 U/mL penicillin, and 0.1 mg/mL streptomycin. As we previously demonstrated that the 3T3 cells show sufficient bone biochemical or morphological characteristic feature after 30 passages. The procedure to determine the proliferation (after 30 passages of MC3T3 cells) on PGD-50 matrix and environment for cell cultural conditions were taken from previously published report.[13] Cell culture was maintained in a gas jacket incubator equilibrated with 5% CO_2 at 37°C. When the cells had grown to confluence, they were digested by 1 mL 0.25% trypsin (Sigma) for 1–2 min, then 3 mL of culture medium were added to stop digestion and the culture medium was aspirated to get cells dispersion, which was used after counting the cells. PGD-50 matrices were sterilized by subsequent cleaning with ethanol in an ultrasonic bath, and then sterile PBS and water. They were placed on the bottom of 24-multiwell dishes and plated with MC3T3 at a density of 2×10^4 cells/cm^2. The cells were harvested from culture flask by trypsin and plated on porous PGD-50 matrix, and the numbers of viable cells were determined at 24, 48, 72, and 96 h by the 3-(4,5-dimethylthiazole-2-yl)-2,5-diphenyltetrzolium bromide (MTT) assay. Porous PGD-50 matrix was transferred into 24-well plates and MTT (5 ng/mL) was added; the matrix was then incubated for 4 h at 37°C. The dye was eluted from the porous PGD-50 matrix with acidified isopropanol, and optical density was measured by a spectrophotometer (Beckman DU-40, Co., Italy) at 570 nm. Porous PGD-50 matrix without cells and medium alone were used as negative controls. The cultured scaffolds were fixed with 4% gluteraldehyde, dehydrated through a series of graded alcohol solution, and then air dried overnight. Dry cellular constructs were sputter coated and observed by Scanning Electron Microscope (bio-LV SEM, SN 3000, Hitachi, Japan).

TABLE II
Compositions, Solvent Ratios, Concentrations, and Spinning Rate of PGD-50 Solutions

Sample	MC/DMF Ratio (w/w)	Solution Concentration (%)	Electrospinning Rate (mL/h)	Range of Fiber Diameter (nm)	Contact Angle (deg)
PGD-50	80/20	25	1.5	350–900	100 ± 7

Applied electric voltage and distance between tip of syringe and collector drum were 15 kV and 12 cm, respectively.

Characterization

^{1}H NMR spectra were recorded with a JNM-Ex 400 FT NMR spectrometer (JEOL Ltd., Japan), in chloroform-d with tetramethylsilane (TMS) as an internal standard. Fourier-transform infrared (FT IR) spectra were recorded as KBR pellets using an ABB Bomen MB100 Spectrometer (Bomen Inc., Canada). The weight average molecular weight (M_w) of the polymer was analyzed by gel permeation chromatography via a Waters 150C (Polymer Laboratories, England) using chloroform as a mobile phase. Thermogravimetric analysis (TGA) was performed by a PerkinElmer TGA 6 (PerkinElmer Inc., USA) under nitrogen atmosphere at a heating rate of 10°C/min and in the range of 50–600°C. Viscosity of the polymer solution was determined by a digital viscometer (D III, Brookfield Co., USA) at 25°C. The morphology of the matrix was examined with bio SEM (Hitachi Co., Japan) after sputter coating with Gold (Au). Pore diameter distribution, total pore volume, pore area, and porosity of the matrix were measured by the Auto Pore IV 9500 V1.05 mercury (Micrometritis Instrument Co., Germany). Mechanical properties were measured with a universal testing machine (AG-5000G, Shimadzu, Japan), under a crosshead speed of 10 mm/min at room temperature. All samples were prepared in the form of standard dumbbell shapes according to ASTM Standard D 638 via die cutting from nonwoven mats and tested in the machine direction. The samples had diameters of 10 mm and thickness of 0.039 mm. The contact angle measurement was carried out by the sessile technique (Digidrop, GBX, France).

RESULTS AND DISCUSSION

PGD synthesis and characterization

Although various silylating agents, such as *N*,*O*-bis (trimethylsilyl) acetamide (BSA), chlorotrimethylsilane (TMSCL), and HMDS have been used for the controlled silylation of polysaccharide, BSA brings on degradation of dextran backbone even at 50°C and TMSCL generates hydrochloric acid (HCL) during silylation and will require undesirable steps. Correspondingly, HMDS can be a best choice for the controlled silylation with the obtainment for high protection yield and protect degradation of dextran chain.[19–22] Under the predetermined conditions, the degree of substitution was found to be 2.5 by the ^{1}H NMR.

After polymerization and successive deprotection in mild acidic condition, graft copolymers were dried under vacuum and characterized by ^{1}H NMR (400 MHz, chloroform-d, TMS) (Fig. 1). The four large peaks that originated from the repeating units of PCL at δ = 1.4 (m, 2H, -CH_2-, poly), 1.6 (m, 4H, -CH_2-, poly), 2.3 (m, -CH_2 C(O)O-, poly), and 4.1 ppm (t, 2H, -CH_2 O(O)C, poly), and one triplet at δ = 3.5 ppm (t, 2H, -CH_2-OH, chain end) were characterized.[23,24] In addition to above peaks, the inclusion of dextran has been confirmed with the appearance of glycosidic protons at δ = 3.7 ppm (m, glycosidic protons). With the formation of core-shell geometry one should expect the masking of dextran with PCL in deuterated chloroform ($CDCl_3$). Therefore, ascertaining the presence of dextran in block copolymer is difficult. But, the finding of glycosidic proton at δ 3.7 ppm realizes to expect it within close proximity with PCL unit. Also, the conformation of glucopyranose residues is crucial to address the fact, as these residues are nearly related by a molecular twofold screw axis.[23].The chains in the form of sheets that are separated by water molecules thereby not acting as hydrophilic moiety.[25,26]

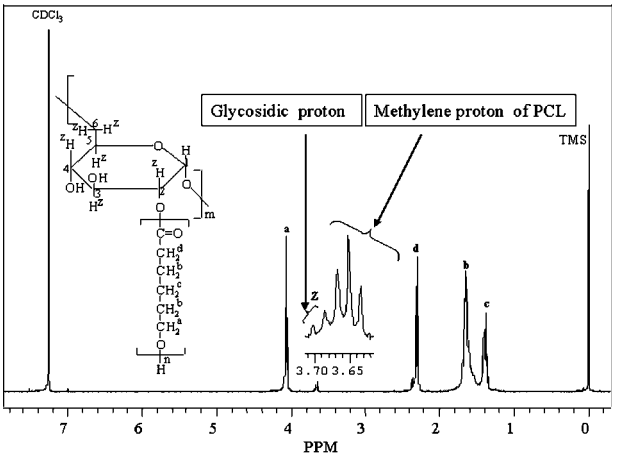

Figure 1 The ^{1}H NMR spectrum ($CDCl_3$) of PGD graft copolymer.

The F_{PCL} in the copolymer was determined with the help of ^{1}H NMR by comparison with the average value of methylene protons of PCL at δ 4.1 ppm and δ 2.35 ppm with the glycosidic methane and methylene protons in the range δ 3.0 to δ 4.0 ppm.[20]

Complete deprotection has been demonstrated by FT IR spectroscopy, the disappearance of absorption bands of the trimethylsilyl functions at the benefit to a large absorption at ca. 3500 cm^{-1} typical of hydroxyl groups. As expected, the six absorption bands related to trimethylsilyl groups, 750 [Si-C, rocking vibration, $Si(CH_3)_3$], 842 [Si-C, rocking vibration, $Si(CH_3)_3$], 874 (Si-O-C, asymmetric stretching), 1020 (Si-O-C, asymmetric stretching) 1156 (O-$(CH_3)_3$, stretching), and 1250 (Si-C, symmetric bending, Si-CH_3) cm^{-1} have been disappeared (Fig. 2).

TGA thermograms (Fig. 3) of the polymers exhibited increment in inflection point temperature (T_d) with increasing OH/ε-CL feed ratio (Table I). Also, T_d value of PGD-20 showed two weight loss steps: the first degradation at 355°C was due to dextran back-

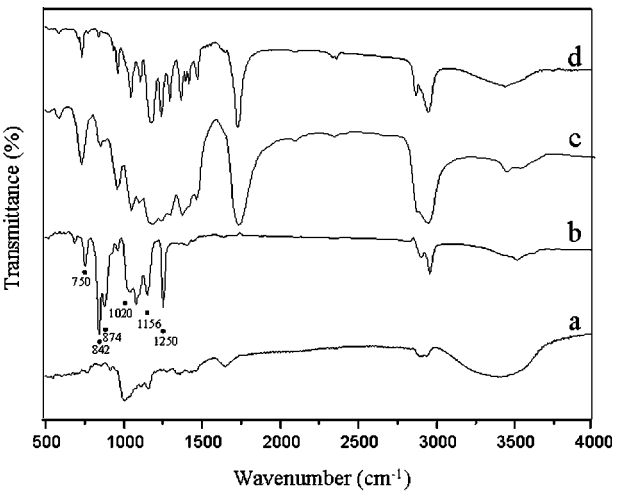

Figure 2 FT IR spectra of PGD graft copolymer.

bone component and the second at 420°C due to the PCL chain. Ciardelli et al.[16] has reported the double degradative phenomena in dextran/PCL blend due to the pyrolysis of individual blend component within the system. But in our synthesized copolymer single degradation is exhibited at 427 and 430°C for PGD-30 and PGD-50, respectively. Results clearly show that synthesized copolymers of PGD favor (faster) degradation than PCL alone and also better than blending system in coherence with Philipe Dubois et al.[27] Pyrolysis of PGD occurred at lower temperature than that of pure PCL, probably as a consequence of interactions occurring between PCL and degradation products from the natural component. We synthesized three different products of PGD (PGD-20, PGD-30, and PGD-50) with different molecular weight.

PGD-50 matrix preparation and characterization

As discussed in earlier literatures,[4,5,28] the control over different electrospinning parameter, such as concentration, molecular weight, conductivity, applied voltage, distance of source electrode from the target substrate, temperature, and solvent volatility has been optimized for the better spinnability. While talking particularly about PGD, we faced the problem with low molecular weight PGD (PGD-20 and PGD-30) that resulted in electrosraying and bead formation. It is due to the breaking up of zet of low molecular fluid into droplets. However, in high molecular weight PGD (PGD-50) with optimization of above all parameters, we did not suffer any difficulties to get fiber. It undergoes a bending instability that causes a whip like motion between the capillary tip and the grounded target so as to produce uniform fiber. It is this bending instability that accounts for the high degree of single fiber drawing, which results in submicron size fibers.[29–31] Although, PGD-50 was soluble in MC at high concentrations the high vapor pressure of it caused rapid solvent evaporation during electrospinning that resulted in plugging of the syringe injection nozzle and even ejecting the droplets. DMF is less volatile than MC; however, the copolymer is not soluble in DMF at high concentrations. Consequently, a mixed solvent of 80/20 w/w MC/DMF resulted in the desired solubility and volatility to facilitate electrospinning. And the use of DMF as a cosolvent increases the spinnability thereby obtaining uniform PGD-50 nanofiber at determined viscosity with optimum porosity and hydrophilicity Table II. In this manner, with several heat and trail selection of solvent ratio, the most uniform fibers derived with our experimental conditions were afforded.[8,12] Further, the viscosity of the solution dissolved in MC/DMF remained as the function of PGD-50 concentration. It was found to increase with increasing concentration and *vice versa*, in agreement with previous study.[8]

Since PCL is hydrophobic in nature, higher the fraction of PCL on PGD matrix, the more hydrophobic surface.[29] As studied by E. Luong-Van et al.,[32] the advancing contact angle of PCL mat is 139° but it was only 77° in case of PCL film.[33] Consistent with the findings of other groups,[34,35] the higher advancing contact angle PCL mats than that of films may be attributed to trapped air within the pores of the mats.[35] In agreement with above study, the contact angle obtained for PGD-50 matrix was 100 ± 7°. Despite, the dextran moiety in PGD-50 is naturally hydrophilic, the hydrophobic properties strongly corroborate the successfully derivatisation (grafting) of dextran by PCL. The hydrophobicity exhibited by the matrix indicates that the outer-most molecular layer of the fiber consists predominantly of PCL.

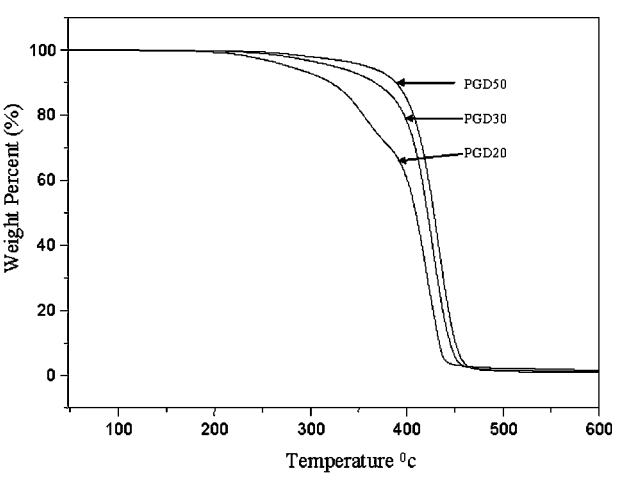

Figure 3 TGA thermograms obtained by heating the samples from 50 to 600°C at 10°C/min under the steady flow of nitrogen (a) PGD-20, (b) PGD-30, and (c) PGD-50.

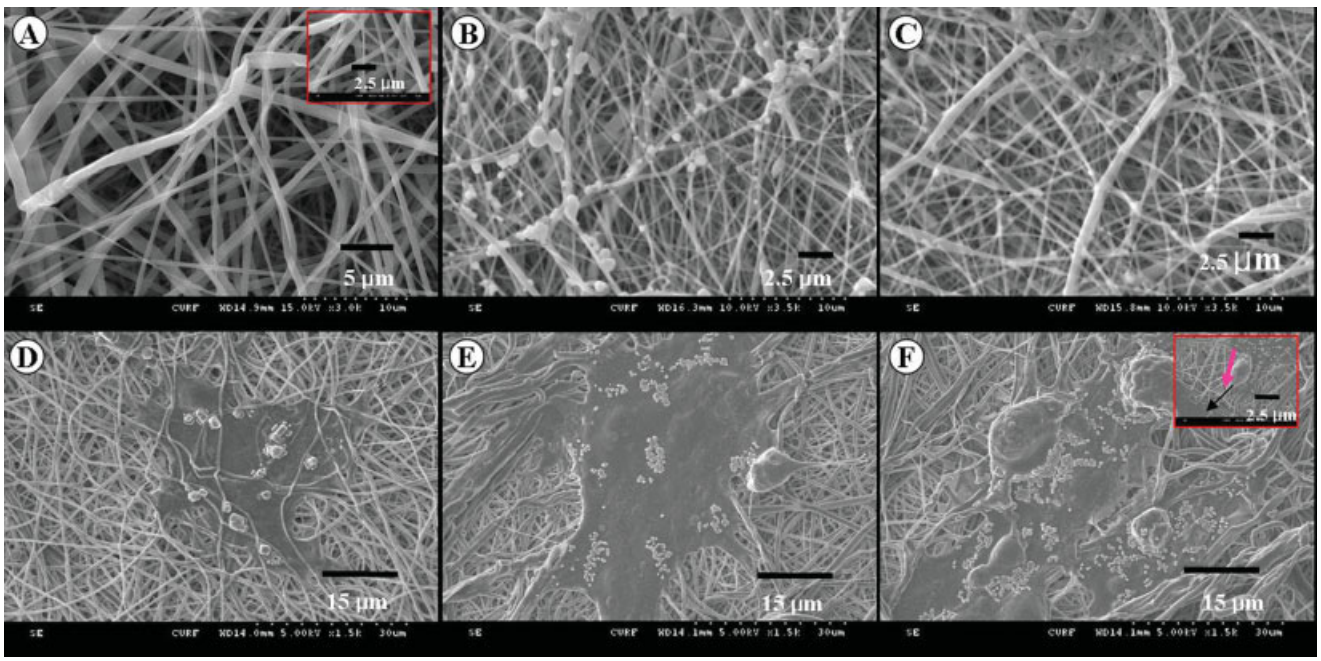

Figure 4 SEM Micrograph of MC3T3 cells seeded on electrospun PGD-50 matrix (A) matrix (5 μm, 3k) prior to seeding with high magnification inset (2.5 μm, 10k). The scaffold has a three-dimensional, interconnected pore structure with average diameter 412nm. (B,C) micrographs (10 μm, 3.5k) of matrix after 3 days and 7 days hydrolytic degradation, showing no degradation of the fiber. (D,F) matrix with MC 3T3 cells after 1 day, 2 days, and 3 days cell culture; magnification and scale bar are 1.5k and 15 μm, respectively. Inset of micrograph F is high magnification (2.5k) of the same and having scale bar with 5 μm. [Color figure can be viewed in the online issue, which is available at www.interscience.wiley.com.]

Parameters such as porosity, micro/macrostructure of the pores and mechanical properties are significant for an ideal synthetic ECM.[3,36–38] Mercury porosimetry analysis demonstrated the porosity of the matrix was about 80–90% with median pore size 7 μm and total pore area 10 m^2/g, indicating the high porosity, Figure 4(A) and Table III. However, the largest pores were up to 100 μm and majority of the pores were less than 10 μm. The matrices showed the maximum broken strength of 2.8 MPa, and the elongation was 148%, Table IV. As a reference point, these mechanical characteristics are smaller than the matrix of triblock PPDO/PLLA-PEG scaffolds,[3] but considerably in the range of matrix of collagen and fibrinogen scaffolds.[7] Besides, the mechanical properties of electrospun nonwoven mats are dependent on structures, such as the geometrical arrangement of the fibers, bond points, and the fiber size and distribution.[39,40]

Biocompatibility and cell-matrix interaction of PGD-50 matrix

An ideally engineered ECM involves sequential events, such as cell attachment, proliferation, differentiation, and deposition of cell matrix proteins.[3,36,37] Several reports indicate that the topographical features of ECM are able to modify cellular biological functions.[3] Result shows that cell proliferation was higher on PGD-50 matrix than that of control PCL matrix in agreement with earlier report.[4,12-13,16] Morphological changes of the PGD-50 matrix with the hydrolytic degradation time were observed by SEM. As in our ongoing work, the degradation has not

TABLE III
Pore Characteristics of the Matrix of PGD-50 Membrane

Sample	Porosity (%)	Total Pore Area (m^2/g)	Pore Diameter Range (μm)	Majority of Pore Diameters (μm)
PGD-50	80–90	10	0.2–200	<105
PLLA/PEG (80/20)	92	15	0.6–360	<100
PLGA[26]	91.6	23.5	2–465	25–100

Results were compared from pore size distribution vs pore diameter observation in the mercury porosity experiment.

TABLE IV
Comparative Study of Mechanical Properties of Electrospun PGD-50 Fibrous Matrix Measured in Dry Conditions With Different Other Scaffolds

Sample	Tensile Modulus (MPa) ± SD	Tensile Strength (MPa) ± SD	Elongation (%) ± SD
PGD-50	200 ± 18	2.8 ± 0.2	148 ± 13
PLLA/PEG (80/20)	400	8	150
PLGA[28]	323	23	96
Cartilage[28]	130	19	20–120
Collagen fiber[26]	26–32	0.7–1.5	–
Fibrinogen[29]	80	2	–

The width, length (gauge), and thickness are 3, 10, and 0.039 mm, respectively.

been started till 7 days in PBS (SEM micrograph 4B and 4C). Detailed study about the degradation of PGD-50 matrix and film is in progress, and will be reported separately.

For tissue engineering, only surface compatibility is not sufficient. Conjointly, it is important to have a three-dimensional structure of scaffold for cell attachment, growth, and migration. SEM micrographs [Fig. 4(D–F)] reveal the micro observation on the cellular response to this structure. In this study, cell matrix interaction (cell spreading) was evaluated in terms of SEM micrograph observation, Figure 4(D–F). The larger the coverage area of the cytoplasm and nucleus by wide spreading cell membrane is, the better the cell spread (grow). Cell morphology and the interaction between cells and matrix were studied *in vitro* for 3 days. MC3T3 mouse osteoblast adhered and spread on the surface of the PGD-50 fiber network and penetrated under the fiber [Fig. 4(D)]. These fibroblasts interacted and integrated well with the surrounding fibers [Fig. 4(E)]. SEM micrographs showed that the development of cell growth was guided by the fiber architecture. Cells grew in the direction of fiber orientation, forming a three-dimensional and multicellular network and slight accumulation in more hydrophobic domain so as to form cell buds [Fig. 4(F)]. Overall, this evidence indicates that nanofibrous structures positively promote cell-matrix and cell-cell interactions, thus regulating signals from matrix and neighbor cells to induce the seeded cells in this structure as to express the phenotypic shape. The increase in cell into twofolds also favors such spreading within three culture days as determined by MTT assay. When the cells adhere onto the specimen surface, the cell spread out and become flattened on the surfaces.[11,12] This is good index to the quality of cell growth in assessing the biocompatibility of implant materials as discussed in our previous publication.[11,12] In this study, cell seeded on the porous scaffold (PGD-50 matrix), [Fig. 4(F)] are found to have appropriate interaction and better cell spreading as can be observed from the SEM images [Fig. 4(D)] that cells penetrates the matrix to some extent, which later spread over the nanomatrix.[3] The reason behind the better cell spreading onto the PGD-50 matrix might be contact guidance phenomenon derived from the influence of material surface topography organized by two different phases (hydrophilic and hydrophobic) on the actin cytoskeleton, focal adhesion, and microtubule of the cells or from the biomechanical equilibrium between cells and materials surface. From this evidence, it indicates that PGD-50 matrix structures positively promote cell-matrix interactions and inter cell communication.

CONCLUSIONS

In this study, we successfully prepared the new matrix of PCL grafted dextran biodegradable polymer for the first time. With all known experimental setup conditions, the fabricated PGD-50 matrix was found highly porous with considerable mechanical properties mimicking to that of ECM. Furthermore, our preliminary results like biocompatibility and cell-matrix interaction of the matrix were highly promising biological indicators, and showed better future direction to be applicable in tissue engineering.

Authors thank profs P. H. Hwang and H. K. Yi for providing bio-lab facilities.

References

1. Jayaraman, K.; Kotaki, M.; Zhang, Y. Z.; Mo, X. M.; Ramakrishna, S. J Nanosci Nanotechnol 2004, 4, 52.
2. Bhattarai, N.; Li, Z.; Edmondson, D.; Zhang, M. Adv Mater 2006, 18, 1463.
3. Bhattarai, S. R.; Bhattarai, N.; Yi, H. K.; Hwang, P. H.; Cha, D. I.; Kim, H. Y. Biomaterials 2004, 25, 2595.
4. Bhattarai, N.; Edmondson, D.; Veiseh, O.; Matsen, F. A.; Zhang, M. Biomaterials 2005, 26, 6176.
5. Khil, M. S.; Cha, D. I.; Kim, H. Y.; Kim, I. S.; Bhattarai, N. J Biomed Mater Res Part B 2003, 67, 675.
6. Ohkawa, K.; Cha, D. I.; Kim, H. Y.; Nishida, A.; Yamamoto, H. Macromol Rapid Commun 2004, 25, 1600.
7. Bhattarai, S. R.; Bhattarai, N.; Viswanathamurthi, P.; Yi, H. K.; Hwang, P. H.; Kim, Y. J Biomed Mater Res Part A 2006, 78, 247.
8. Khil, M. S.; Bhattarai, S. R.; Kim, H. Y.; Kim, S. Z.; Lee, K. H. J Biomed Mater Res Part B 2005, 72, 117.
9. Bhattarai, N.; Cha, D. I.; Bhattarai, S. R.; Khil, M. S.; Kim, H. Y. J Polym Sci Part B: Polym Phys 2003, 41, 1955.
10. Kim, C. H.; Khil, M. S.; Kim, H. Y.; Lee, H. U.; Jahng, K. Y. J Biomed Mater Res Part B 2006, 78, 283.
11. Li, W. J.; Laurencin, C. T.; Caterson, E. J.; Tuan, R. S.; Ko, F. K. J Biomed Mate Res Part A 2002, 60, 613.
12. Loesberg, W. A.; Walboomers, X. F.; Van Loon, J. J. W. A.; Jansen, J. A. Cell Motility Cytoskeleton 2006, 63, 384.
13. Cai, Q.; Wan, Y.; Bei, J.; Wang, S. Biomaterials 2003, 24, 3555.

14. Peter, S. J.; Miller, M. J.; Yasko, A. W.; Yaszemski, M. J.; Mikos, A. G. J Biomed Mater Res Part B 1998, 43, 422.
15. Lindahl, U.; Höök, M. Annu Rev Biochem 1978, 47, 385.
16. Ciardelli, G.; Chiono, V.; Vozzi, G.; Pracella, M.; Ahluwalia, A.; Barbani, N.; Cristallini, C.; Giusti, P. Biomacromolecules 2005, 6, 1961.
17. Takasu, A.; Takada, M.; Itou, H.; Hirabayashi, T.; Kinoshita, T. Biomacromolecules 2004, 5, 1029.
18. Lee, Y.; Koo, H.; Jin, G. W.; Mo, H.; Cho, M. Y.; Park, J. Y.; Choi, J. S.; Park, J. S. Biomacromolecules 2005, 6, 24.
19. Ydens, I.; Delphine, R.; Philippe, D.; Six, J. L.; Dellacherie, E.; Dubois, P. Macromolecules 2000, 33, 6713.
20. Nouvel, C.; Dubois, P.; Dellacherie, E.; Six, J. L. J Polym Sci Part A: Polym Chem 2004, 42, 2577.
21. Nouvel, C.; Ydens, I.; Degee, P.; Dubois, P.; Dellacherie, E.; Six, J. L. Polymer 2002, 43, 1735.
22. Riva, R. I.; Schmeits, S.; Jerome, C. R.; Lecomte, P. Macromolecules 2007, 40, 796.
23. Nouvel, C.; Dubois, P.; Dellacherie, E.; Six, J. L. Biomacromolecules 2003, 4, 1443.
24. Aryal, S.; Bahadur, K. C. R.; Bhattarai, N.; Lee, B. M.; Kim, H. Y. Mater Chem Phys 2006, 98, 463.
25. Guizard, C.; Chanzy, H.; Sarko, A. J Mol Bio 1985, 183, 397.
26. Kim, K.; Yu, M.; Zong, X.; Chiu, J.; Fang, D.; Seo, Y. S.; Hsiao, B. S.; Chu, B.; Hadjiargyrou, M. Biomaterials 2003, 24, 4977.
27. Dubois, P.; Narayan, R. Macromol Symp 2003, 198, 233.
28. Bhattarai, S. R.; Khalil, K. A.; Dewidar, M. P.; Hwang, H.; Yi, H. K.; Kim, H. Y. J Biomed Mater Res Part A, to appear.
29. Wnek, G. E.; Carr, M. E.; Simpson, D. G.; Bowlin, G. L. Nano Lett 2003, 3, 213.
30. Jones, D. S.; Djokic, J.; McCoy, C. P.; Gorman, S. P. Biomaterials 2002, 23, 4449.
31. Hafren, J.; Cordova, A. Macromol Rapid Commun 2005, 26, 82.
32. Luong-Van, E.; Grondahl, L.; Chua, K. N.; Leong, K. W.; Nurcombe, V.; Cool, S. M. Biomaterials 2006, 27, 2042.
33. Lim, J. Y.; Liu, X.; Vogler, E. A.; Donahue, H. J. J Biomed Mater Res 2004, 68, 504.
34. Zhang, Y.; Ouyang, H.; Lim, C. T.; Ramakrishna, S.; Huang, Z. M. J Biomed Mater Res B: Appl Biomater 2005, 72, 156.
35. Fujihara, K.; Kotaki, M.; Ramakrishna, S. Biomaterials 2005, 26, 4139.
36. Cho, C. S.; Seo, S. J.; Park, I. K.; Kim, S. H.; Kim, T. H.; Hoshiba, T.; Harada, I.; Kaike, T. Biomaterials 2006, 27, 576.
37. Pan, H.; Jiang, H.; Chen, W. Biomaterials 2006, 27, 3209.
38. Aryal, S.; Bajgai, M. P.; Khil, M. S.; Kang, S.; Kim, H. Y. J Biomed Mater Res Part A, to appear.
39. McKee, M. G.; Wilkes, G. L.; Colby, R. H.; Long, E. T. Macromolecules 2004, 37, 1760.
40. Lee, K. H.; Kim, H. Y.; La, Y. M.; Lee, D. R; SUNG, N. H. J Polym Sci Part B: Polym Phys 2002, 40, 2259.